European Radiology (2019) 29:2069–2078
https://doi.org/10.1007/s00330-018-5736-0

COMPUTED TOMOGRAPHY

How accurate and precise are CT based measurements of iodine concentration? A comparison of the minimum detectable concentration difference among single source and dual source dual energy CT in a phantom study

André Euler[1] · Justin Solomon[2] · Maciej A. Mazurowski[1] · Ehsan Samei[2] · Rendon C. Nelson[1]

Received: 20 June 2018 / Revised: 9 August 2018 / Accepted: 28 August 2018 / Published online: 1 October 2018

Abstract

Objectives To assess the impact of scan- and patient-related factors on the error and the minimum detectable difference in iodine concentration among different generations of single-source (SS) fast kV-switching and dual-source (DS) dual-energy CT (DECT).

Methods Lesions having eight different iodine concentrations (0.2–4 mgI/mL) were emulated in a 3D-printed phantom of medium and large size. Each combination of concentration and size was scanned in dual-energy mode on four different SS and DS DECTs. Radiation doses were 7 and 10 mGy (medium size) and 10, 13, and 16 mGy (large size). Iodine maps were reconstructed with filtered back projection (FBP) and vendor-specific iterative reconstruction algorithms (IRs). Absolute error of iodine quantification (E) was measured. Multivariate regression models determined the influence of CT scanner, iodine concentration, phantom size, radiation dose, and reconstruction algorithm on E. The minimum detectable difference in iodine concentration (IC_{min}) under the same imaging conditions (intra-conditional) and among different imaging conditions (inter-conditional) was calculated.

Results The error was significantly lower in current than in previous DECT generations ($p < 0.001$). For all CT scanner conditions, the error was significantly higher with increasing phantom size and decreasing radiation dose ($p < 0.001$). Iodine concentration only significantly affected the error for SS DECT ($p < 0.001$). IC_{min} depended on patient- and scan-related factors and ranged from 0.4 to 1.5 mgI/mL.

Conclusions Patient- and scan-related factors have a significant impact on the error and minimum detectable difference in iodine concentration within and among SS fast kV-switching and DS DECT.

Key Points

- *Patient- and scan-related factors have a significant impact on the error and minimum detectable difference in dual-energy CT-based iodine quantification.*
- *Third-generation DECTs outperformed second-generation scanners for both single-source and dual-source dual-energy CT.*
- *The minimum intra- and inter-conditional detectable difference in iodine concentration ranged from 0.4 to 1.5 mg iodine/mL.*

Keywords Multidetector computed tomography · Iodine · Phantom imaging

Electronic supplementary material The online version of this article (https://doi.org/10.1007/s00330-018-5736-0) contains supplementary material, which is available to authorized users.

✉ André Euler
and.euler@gmail.com

[1] Department of Radiology, Duke University Medical Center, 2301 Erwin Road, Box 3808, Durham, NC 27710, USA

[2] Carl E. Ravin Advanced Imaging Laboratories, Durham, NC, USA

Abbreviations

DECT	Dual-energy computed tomography
DECT-IQ	Dual-energy CT-based iodine quantification
DS	Dual-source
FBP	Filtered back projection
IC_{min}	Minimum detectable difference in iodine concentration
IR	Iterative reconstruction algorithm
IRB	Institutional review board

RCC Renal cell carcinoma
SS Single-source

Introduction

Dual-energy CT-based iodine quantification (DECT-IQ) has been shown to improve lesion detection and characterisation and to enable monitoring of tumour treatment response in oncologic imaging of the abdomen and pelvis [1–6]. Several clinical studies demonstrated its capability to distinguish malignant from benign lesions [7, 8] as well as metastatic from non-metastatic lymph nodes [9]. Recently, the potential for DECT-IQ as a predictive pre- and post-treatment imaging biomarker has been investigated [10, 11]. Additional benefits have been observed in the response assessment of different cancer entities that are treated with targeted antiangiogenetic therapy [12, 13]. Here, DECT-IQ can be used as a quantitative tool to assess tumour vascularisation in order to distinguish responders from non-responders [12]. DECT-IQ must be precise and reproducible to ensure accurate diagnosis of disease as well as interpretation of tumour treatment response in oncologic patients. However, recent clinical studies have shown contradictory results regarding the thresholds of iodine concentration that should be used for lesion characterisation. A recent study reported a threshold of 1.9 milligram iodine per millilitre (mgI/mL) to differentiate between benign and malignant renal lesions with the latter demonstrating higher iodine concentrations [14]. In a previous study, however, a threshold of 0.9 mI/mL enabled the discrimination between clear cell and papillary renal cell carcinoma (RCC) [15]. Papillary RCCs had a mean lesion iodine concentration of 0.8 ± 0.1 mgI/mL. Thus, by applying the most recent threshold [14], these lesions would have been inaccurately characterised as benign. This discrepancy could be explained by either the application of different amounts of contrast medium or by the use of different DECT scanners. The initial study was performed on a second-generation dual-source (DS) DECT, while the latter used a second-generation single-source (SS) fast kV-switching DECT. This raises the question: to what extent is iodine quantification biased by patient- or scan-related factors? Although multiple former studies have investigated the accuracy of DECT-based iodine quantification [2, 16–23], it remains unclear which inaccuracies should be expected if (A) the same patient or (B) different patients of different habitus are imaged under the same or different imaging conditions. Based on this lack of knowledge, Jacobsen et al recently proposed that future work should include the determination of the minimum detectable iodine concentration (IC_{min}) to compute the error margin for each specific DECT platform [20].

The purpose of our study was to assess the impact of patient- and scan-related factors on the accuracy and precision of DECT-IQ and to determine the minimum detectable difference in iodine concentration for different generations of SS fast kV-switching and DS DECT.

Materials and methods

Phantom design

A custom abdominal phantom was fabricated using a 3D printer. The phantom was composed of a large hollow chamber with a volume of 1.9 litres and a lid containing 15 fillable cylinders (8 cm length in the z-direction) of different diameters (5–20 mm) to simulate variously sized focal lesions (Fig. 1). The chamber was filled with distilled water and all cylinders were filled with iodinated solutions of eight different concentrations (0.2, 0.4, 0.6, 0.8, 1.0, 1.2, 2.4, and 4 mg iodine per mL [mgI/mL]). The iodinated solutions were prepared by mixing distilled water with iopamidol (300 mgI/mL, Isovue-300, Bracco Diagnostics). One (4 cm total) or two (8 cm total) peripheral rings of fat-equivalent material were added to simulate medium- and large-sized patients, respectively (Fig. 1).

Scan setup

Each combination of iodine concentration and phantom size was scanned three times in dual-energy mode using the following five different CT scanner conditions: (A) a second-generation SS fast kV-switching DECT (Discovery 750HD, GE Healthcare); (B) a third-generation SS fast kV-switching DECT (Revolution CT, GE Healthcare); (C) a second-generation DS DECT at a tube voltage combination of 100 kV and 140 kV with tin filtration (100/Sn140) (Somatom Definition Flash, Siemens Healthineers); (D) a third-generation DS DECT at 100/Sn150 (Somatom Force, Siemens Healthineers); and (E) a third-generation DS DECT at 80/Sn150 (Somatom Force, Siemens Healthineers).

Radiation dose levels ($CTDI_{vol}$) were 7 and 10 mGy in the medium phantom and 10, 13, and 16 mGy in the large phantom. Vendor-specific scan protocols were applied to simulate a common scenario in routine clinical practice. To achieve the desired radiation dose levels, predefined scan pre-sets had to be chosen for both SS fast kV-switching DECTs while the tube current had to be adjusted for the DS DECTs (see Table 1). Datasets were reconstructed with both FBP and scanner-specific iterative reconstruction algorithms (IRs).

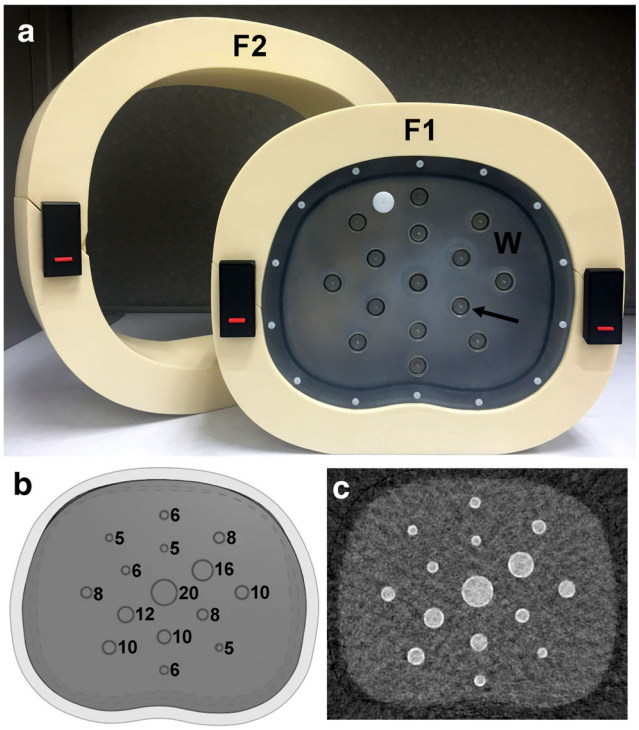

Fig. 1 Custom-made, 3D-printed abdominal phantom. **a** The phantom consists of a fillable chamber (W) and 15 fillable cylinders (black arrow) with diameters of 5–20 mm (the 5-mm and 6-mm cylinders were excluded from the analysis). The chamber was filled with distilled water and the cylinders with iodinated solutions of different concentrations. One (*F1*) or two (*F2*) rings of fat-equivalent material were applied to simulate medium- and large-sized patients. **b** Schematic drawing of the phantom demonstrating the distribution of the different cylinder sizes. **c** Iodine map with all cylinders filled with an iodine concentration of 4.0 mgI/mL

Overall, 600 different CT scans (5 CT scanner conditions x 5 combinations of radiation dose and size x 8 iodine concentrations x 3 repeats) were performed and 1200 CT datasets were reconstructed (2 reconstruction algorithms). All CT scans for a certain iodine concentration were performed during the same session. Each session was separated by 1 week. Each CT scanner was calibrated in air immediately before scanning each setup. Iodine maps were created for each dataset on separate vendor-specific software packages (AWServer2, GE Healthcare and Syngo.via, VA20, Siemens Healthineers). For each of those reconstructions, a section thickness of 5 mm with an increment of 2.5 mm was used.

Measurement of iodine concentration

The iodine concentration was measured by drawing circular regions of interest (ROIs) within each cylinder on ten contiguous axial sections in the centre of each dataset. A software solution (MATLAB, The MathWorks Inc.) was used to write an automated script to standardise the position and size of the ROIs among all datasets. We chose to exclude the 5-mm and 6-mm cylinders from analysis in order to minimise potential measurement errors produced by the wall of the cylinders. The diameter of each ROI was 4 mm (area = 12.6 mm^2) including approximately 330 pixels. The measured pixel values for each ROI in the exported DICOM iodine-water maps had to be converted into units of iodine concentration (in mgI/mL). This conversion is vendor-specific (see Appendix A1).

Quantitative assessment of iodine quantification error

For each ROI, an absolute error of iodine quantification (E) was computed as: |E| = |real iodine concentration - measured concentration|. The absolute error was averaged across all 90 ROIs for each dataset. These measurements were used to establish whether the association between the E was associated with the CT scanner condition. We conducted analysis of variance (ANOVA) followed by a Tukey honest significant differences (HSD) test to establish significance of pairwise differences across different CT scanner conditions. In a subanalysis by CT scanner condition, we constructed multivariate linear regression models with the individual variables (iodine concentration, phantom size, radiation dose, and reconstruction algorithm) as the model input and the absolute error as the dependent variable in order to determine whether the individual variables were associated with the error of iodine quantification. This enabled establishing the impact of each variable on error while controlling for other variables. A statistical software (R, version 3.3.2, R Foundation for Statistical Computing) was used for the analysis.

Estimation of minimum detectable difference in iodine concentration among different imaging conditions

Individual measurements of iodine concentration from DECT images are inherently associated with some degree of uncertainty due to many factors such as image noise, image artifacts, variable scanner capabilities, and variable patient characteristics. Given this uncertainty, how can one know if a *measured* difference in iodine concentration corresponds to a *true* difference? This analysis attempted to answer that question by using the large number of measurements described in the previous sections and statistically estimating the minimum measured difference in iodine concentration that reliably corresponds to a true difference.

This statistical analysis is described briefly below and in detail in Appendix A2. Consider the case where two measurements of iodine concentration, m_A and m_B, have been made from images acquired under different imaging conditions, A and B. Here, an imaging condition corresponds to an unique combination of patient- and scan-related factors (CT scanner condition, phantom/patient size, radiation dose level, and

Table 1 Scan parameters of all five CT scanner conditions

A) Second-generation SS fast kV-switching DECT

Setup	Phantom size	Radiation dose (mGy)	Tube voltage (kVp)	Tube current (mA)	Collimation width (mm)	Total collimation width (mm)	Rotation time (s)	Pitch
1	M	7	80/140	275	0.625	40	0.6	1.375
2	M	10	80/140	375	0.625	40	0.7	1.375
3	L	10	80/140	375	0.625	40	0.7	1.375
4	L	13	80/140	630	0.625	40	0.5	1.375
5	L	16	80/140	375	0.625	40	0.7	1.375

B) Third-generation SS fast kV-switching DECT

Setup	Phantom size	Radiation dose (mGy)	Tube voltage (kVp)	Tube current (mA)	Collimation width (mm)	Total collimation width (mm)	Rotation time (s)	Pitch
1	M	7	80/140	320	0.625	40	0.6	1.375
2	M	10	80/140	440	0.625	40	0.6	1.375
3	L	10	80/140	440	0.625	40	0.6	1.375
4	L	13	80/140	440	0.625	40	0.8	1.375
5	L	16	80/140	435	0.625	40	1.0	1.375

C) Second-generation DS DECT

Setup	Phantom size	Radiation dose (mGy)	Tube voltage (kVp)	Tube current (mA)	Collimation width (mm)	Total collimation width (mm)	Rotation time (s)	Pitch
1	M	7	100/Sn140	78	0.6	19.2	0.5	0.6
2	M	10	100/Sn140	155	0.6	19.2	0.5	0.6
3	L	10	100/Sn140	155	0.6	19.2	0.5	0.6
4	L	13	100/Sn140	186	0.6	19.2	0.5	0.6
5	L	16	100/Sn140	232	0.6	19.2	0.5	0.6

D) Third-generation DS DECT at 100/Sn150

Setup	Phantom size	Radiation dose (mGy)	Tube voltage (kVp)	Tube current (mA)	Collimation width (mm)	Total collimation width (mm)	Rotation time (s)	Pitch
1	M	7	100/Sn150	60	0.6	76.8	0.5	0.6
2	M	10	100/Sn150	86	0.6	76.8	0.5	0.6
3	L	10	100/Sn150	86	0.6	76.8	0.5	0.6
4	L	13	100/Sn150	112	0.6	76.8	0.5	0.6
5	L	16	100/Sn150	138	0.6	76.8	0.5	0.6

E) Third-generation DS DECT at 80/Sn150

Setup	Phantom size	Radiation dose (mGy)	Tube voltage (kVp)	Tube current (mA)	Collimation width (mm)	Total collimation width (mm)	Rotation time (s)	Pitch
1	M	7	80/Sn150	97	0.6	76.8	0.5	0.6
2	M	10	80/Sn150	139	0.6	76.8	0.5	0.6
3	L	10	80/Sn150	139	0.6	76.8	0.5	0.6
4	L	13	80/Sn150	181	0.6	76.8	0.5	0.6
5	L	16	80/Sn150	222	0.6	76.8	0.5	0.6

Sn corresponds to the use of a tin filter (Sn) for the second tube in DS DECT. The tube current for the second tube is indicated for the DS DECTs

reconstruction algorithm). Let the measured difference be $\Delta m_{A,\,B} = m_A - m_B$ and the true difference be $\Delta t_{A,\,B} = t_A - t_B$ where t_A and t_B are the corresponding true iodine concentrations. Given the statistical distribution of $\Delta m_{A,\,B}$ and the relationship between $\Delta m_{A,\,B}$ and $\Delta t_{A,\,B}$, it is possible to determine the minimum measurable difference, $\Delta m_{A,\,B,\,min}$, for which $\Delta t_{A,\,B} > 0$, 95% of the time. This minimum measured difference can also be put in terms of the corresponding minimum detectable true difference, $\Delta t_{A,\,B,\,min}$ or IC_{min} (by using the relationship between $\Delta m_{A,\,B}$ and $\Delta t_{A,\,B}$). $\Delta t_{A,\,B,\,min}$ is most appropriate to determine which imaging conditions result in more precise measurements while $\Delta m_{A,\,B,\,min}$ is more useful if one has made two measurements and needs to determine if their difference is likely to correspond to a true difference in iodine concentration.

Both $\Delta m_{A,\,B,\,min}$ and $\Delta t_{A,\,B,\,min}$ were estimated for each pair of imaging conditions, including both intra- (A = B) and inter-comparisons (A ≠ B). 95% confidence intervals were also calculated for these estimates as described in Appendix A2.

Results

Quantitative assessment of iodine concentration error

The ANOVA revealed that E was associated with the CT scanner condition ($p < 0.001$). The Tukey HSD test (pairwise comparison of individual conditions) demonstrated significantly higher mean errors in second-generation DECTs (A and C in Fig. 2) compared to third-generation DECTs (B, D, and E in Fig. 2) for both dual-energy approaches ($p < 0.001$). When averaged over all conditions, the mean error was 0.44 ± 0.24 mgI/mL for second-generation SS DECT, 0.44 ± 0.13 mgI/mL for second-generation DS DECT, 0.28 ± 0.13 mgI/mL for third-generation SS DECT, 0.24 ± 0.07 mgI/mL for third-generation DS DECT at 100/Sn150, and 0.28 ± 0.1 mgI/mL for third-generation DS DECT at 80/Sn150 (Fig. 2). There was no significant difference between the second-generation SS DECT and the second-generation DS DECT (0.44 ± 0.24 mgI/mL vs. 0.44 ± 0.13 mgI/mL; $p = 0.18$). Furthermore, there was no significant difference between the third-generation SS DECT and the third-generation DS DECT at 80/Sn150 (0.28 ± 0.13 mgI/mL vs. 0.28 ± 0.1 mgI/mL; $p = 0.999$). However, third-generation DS DECT at 100/Sn150 demonstrated a significantly lower mean error compared to third-generation SS DECT and third-generation DS DECT at 80/Sn150 (both $p < 0.008$).

A) Single-source DECT

The multivariate regression models showed that the absolute error was significantly associated with iodine concentration, phantom size, and radiation dose for both scanner generations (all $p < 0.001$; see Table A3 of Appendix A3). The reconstruction algorithm only had a significant impact on the second-generation SS DECT ($p < 0.006$), while there was no significant impact on the third-generation SS DECT ($p = 0.373$).

Analysis of the individual variables showed that the error was higher with increasing iodine concentration, and phantom size and was lower with increasing radiation dose (see A1–3 and B1–3 of Fig. 3). This effect was more pronounced in the second-generation DECT. For instance, the mean error increased by 0.47 mgI/mL in the second-generation DECT and by 0.28 mgI/mL in the third-generation DECT when increasing the iodine concentration from 0.2 mgI/mL to 4.0 mgI/mL. When changing the phantom size from medium to large, the mean error increased by 0.3 mgI/mL in the second-generation DECT but only by 0.06 mgI/mL in the third-generation DECT. For the second-generation SS DECT, the error decreased slightly by 0.02 mgI/mL as compared to FBP when applying IR (A4 of Fig. 3).

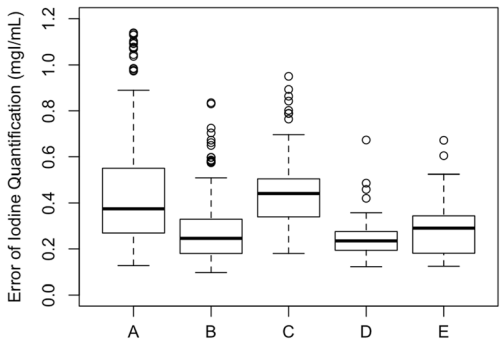

Fig. 2 Boxplots of the mean error of iodine quantification for each of the five different CT scanner conditions. Pairwise comparison of the individual conditions demonstrated significantly higher mean errors in second-generation DECTs (A, C) compared to third-generation DECTs (B, D, and E). A = second-generation SS DECT; B = third-generation SS DECT; C = second-generation DS DECT (100/Sn140); D = third-generation DS DECT (100/Sn150); and E = third-generation DS DECT (80/Sn150)

B) Dual-source DECT

The multivariate regression models demonstrated that the absolute error was significantly associated with the phantom size and radiation dose for both second- and third-generation DS DECTs. The reconstruction algorithms had a significant impact only on the second-generation and the third-generation DS DECT at 100/Sn150 (all $p < 0.001$), while being non-significant for the third-generation CT scanner at 80/Sn150 ($p = 0.06$). There was no significant association between the iodine concentration and the error for both generations ($p > 0.06$).

Analysis of the individual variables showed that the error increased slightly with increasing iodine concentration only for the second-generation DS DECT while there was no increase for both third-generation DS DECTs (see C1, D1, and E1 of Fig. 3). The error was higher with increasing phantom size and lower with increasing radiation dose (C2–3, D2–3, and E2–3). For instance, the mean error increased by 0.18 mgI/mL in the second-generation DS DECT, by 0.10 mgI/mL in the third-generation DS DECT at 100/Sn150, and by 0.16 mgI/mL in the third-generation DS DECT at 80/Sn150 when increasing the phantom size from medium to large. With the application of IR, the mean error decreased slightly by 0.05 mgI/mL in the second-generation DS DECT, by 0.02 mgI/mL in the third-generation DS DECT at 100/Sn150, and by 0.01 mgI/mL in the third-generation DS DECT at 80/Sn150.

Estimation of minimum detectable difference in iodine concentration among different imaging conditions

Figures 4, 5, 6, and 7 of Appendix A4 show the results of the analysis in terms of the minimum *measured* difference in iodine concentration $\Delta m_{A,\,B,\,min}$ (Figs. 4 and 6) and the minimum *detectable* difference in iodine concentration $\Delta t_{A,\,B,\,min}$

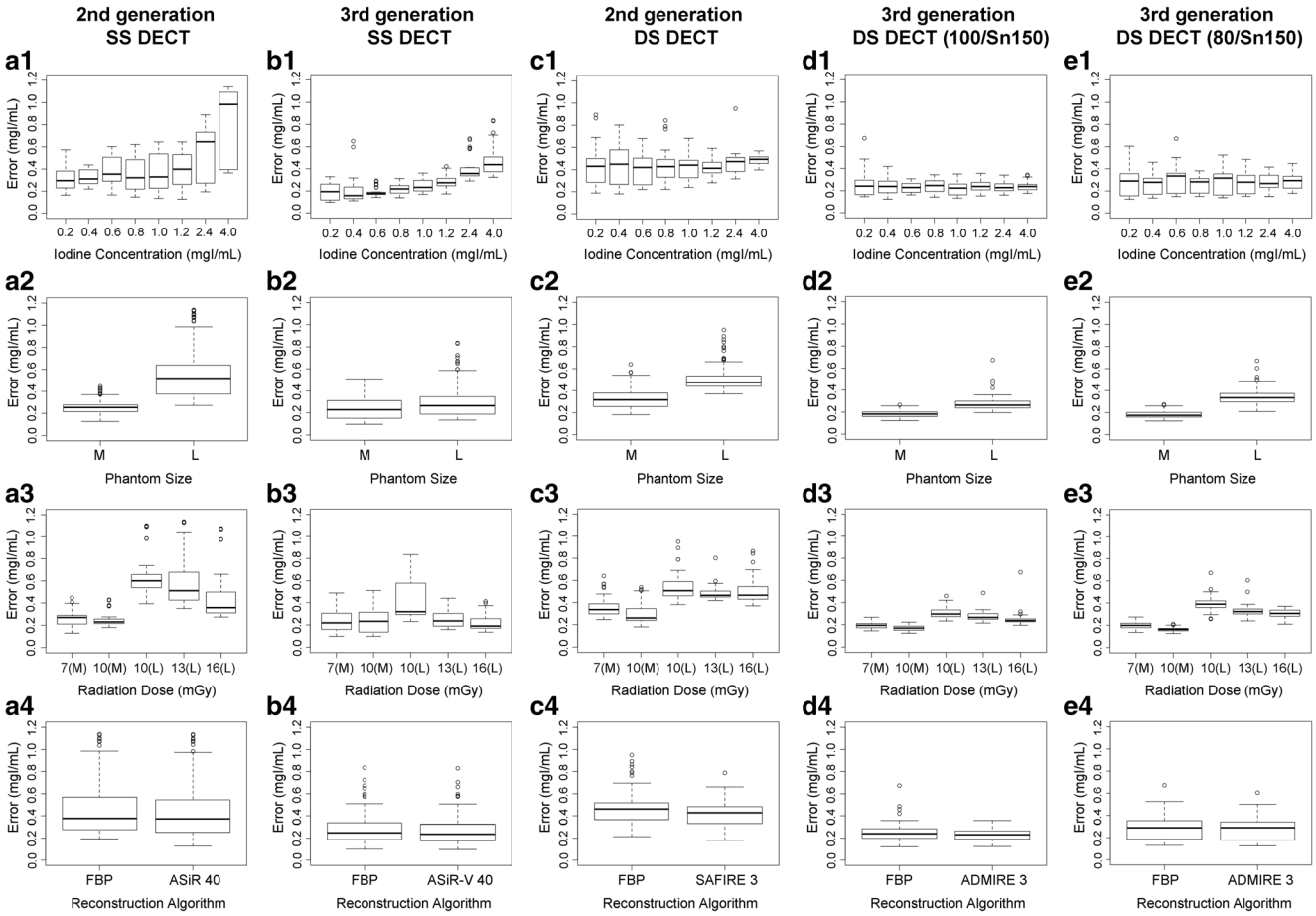

Fig. 3 Boxplots of the mean error of iodine quantification for each CT scanner condition subdivided by patient- and scan-related factors. Phantom size and radiation dose were significantly associated with the error for all five CT scanner conditions. Note the significant impact of iodine concentration on error for SS DECT which was distinct different from the DS DECT platforms

(Figs. 5 and 7). Figures 4 and 5 show bar plots of $\Delta m_{A,\,B,\,min}$ and $\Delta t_{A,\,B,\,min}$, respectively, for the special case where A = B (i.e., intra-conditional). Figures 6 and 7 (Appendix A4) show the same as a heat map for all combinations of conditions present in the data (i.e., inter-conditional).

For intra-conditional cases (A = B), $\Delta m_{A,\,B,\,min}$ and $\Delta t_{A,\,B,\,min}$ mainly depended on the CT scanner model, patient size, and radiation dose. Both $\Delta m_{A,\,B,\,min}$ and $\Delta t_{A,\,B,\,min}$ tended to be lower for the third-generation DECTs compared to the second-generation scanners (under otherwise similar imaging conditions). This was true for both SS and DS DECT systems and implies that the newer scanner models were able to detect smaller changes in iodine concentration compared to the older models. Overall, IC_{min} was smaller when decreasing the patient size and increasing the radiation dose. As an example, IC_{min} decreased from 1.19 ± 0.05 mgI/mL to 0.61 ± 0.03 mgI/mL when increasing the radiation dose from 10 to 16 mGy in the large phantom for the third-generation SS DECT (scanner B). Iterative reconstruction only showed a minor reduction of IC_{min} compared to FBP for all CT scanner conditions.

Discussion

In our study, we assessed the impact of scan- and patient-related factors on the accuracy and precision of DECT-IQ for second- and third-generation SS fast kV-switching and DS DECT. The investigation of very low iodine concentrations allowed us to calculate the IC_{min} that, in 95% of cases, corresponded to an actual difference in iodine concentration unrelated to patient- or scan-related factors. IC_{min} was defined for scans under the same imaging condition (intra-conditional) as well as for scans of two different conditions (inter-conditional).

Our results revealed multiple findings. Current DECT generations outperformed previous generations for both DECT platforms. IC_{min} was up to 50% lower in third-generation scanners. Radiation dose level and simulated patient size had a major influence on IC_{min}, with decreasing values at increasing radiation dose level and smaller patient size. Overall, SS DECT showed comparable IC_{min} compared to DS DECT for both scanner generations. The major differences were higher IC_{min} values for both SS generations at the lowest radiation dose of 10 mGy in the large phantom. Interestingly, IRs showed only a

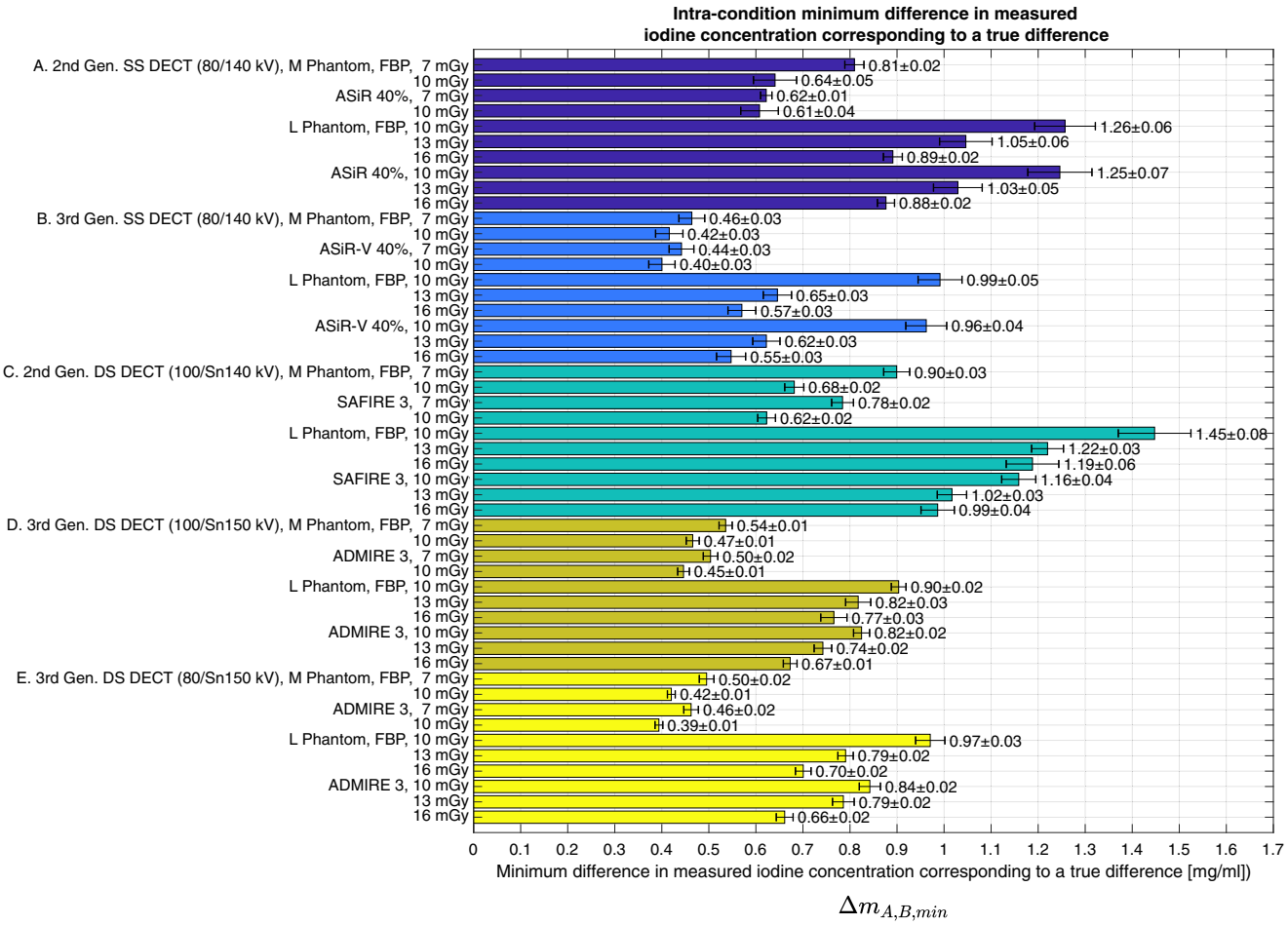

Fig. 4 Detailed bar plots showing the mean with standard deviation of the minimum measurable difference in iodine concentration for each investigated imaging condition (intra-conditional)

minor improvement of the average error compared to FBP for all CT scanner conditions. However, IRs demonstrated consistently lower IC_{min} compared to FBP. This improvement was stronger for DS DECT and only minimal for SS DECT platforms. The observed differences in the quantification error and IC_{min} are most likely attributed to differences in image noise among the scan conditions. Furthermore, technical advances in third-generation scanners (e.g., more efficient detectors, improved image reconstruction, and potentially improved spectral x-ray properties) may contribute to improved DECT-IQ compared to the second-generation.

Overall, the IC_{min} for intra- as well as inter-conditional comparisons ranged between 0.4 and 1.5 mgI/mL. Radiologists should be aware of these relatively high error margins considering the reported small differences in iodine concentration between normal and pathologic conditions [7, 9, 11, 14, 24–26]. Kim et al recently proposed a threshold of 0.4 mg/mL for a truly enhancing lesion in a chest phantom [22]. This number appears to be overly optimistic given our data. From a clinical standpoint, it is important to be aware of the relatively high IC_{min} values in large patients, especially in the second-generation DECTs. These may explain the contradictory results of the two studies mentioned in the introduction section which defined thresholds of DECT-IQ for benign and malignant renal lesions (but were performed on different second-generation DECTs) [14, 15].

Furthermore, we investigated the impact of iodine concentration, patient size, radiation dose, and reconstruction algorithm on the error of iodine quantification for each CT scanner condition. Patient size and radiation dose were the most important factors and had a significant impact on the error for all five scanner conditions. Increased error with phantom size has been described previously in literature [16, 23]. Sauter et al reported a considerable impact of phantom size on error at low radiation dose levels in dual-layer (DL) DECT. The authors observed a decreasing impact as the radiation dose increased [23]. The same tendency was observed in our data. Nevertheless, our results are in contrast to the study by Chandarana et al which did not find significant error differences among phantoms with lateral diameters of 25, 30, and 35 cm [2]. Furthermore, our results differ from the study by Kim et al who reported no significant influence of radiation dose on iodine quantification for SS, DS, and DL DECTs. However, this investigation was performed using a chest

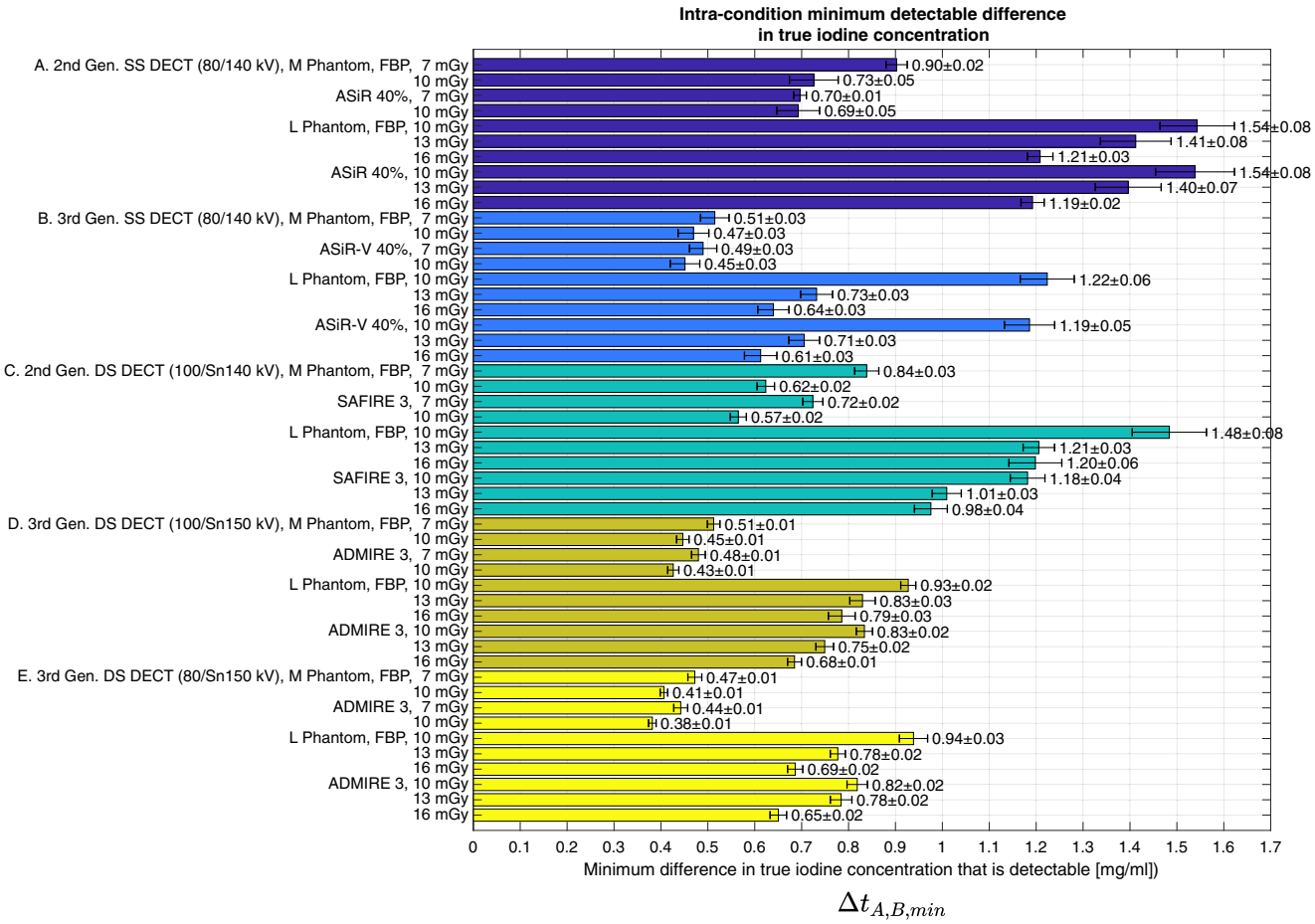

Fig. 5 Detailed bar plots showing the mean with standard deviation of the minimum detectable difference in iodine concentration for each investigated imaging condition (intra-conditional)

phantom, considerably higher iodine concentrations, and only two different radiation dose settings. Interestingly, our study found that iodine concentration significantly affected the error only for the SS DECTs, with increasing error at higher iodine concentrations. This was distinctly different from the DS DECTs. In addition, the application of IRs only minimally decreased the error for all five CT platforms. The same observation has been reported for IR of DL DECT [23].

Another interesting finding was that the kV combination of 100/Sn150 outperformed the kV combination of 80/Sn150 in the third-generation DS DECT. This was mainly due to higher mean errors in the large phantom at 80/Sn150. In theory, a kV setting of 80/Sn150 improves the spectral separation and should therefore decrease quantification errors. Our results demonstrated, however, that this improvement is negated when this setting is used in large-sized patients. We recommend using 100/Sn150 as the default setting in clinical routine and to consider 80/Sn150 only in small- to medium-sized patients.

Overall, the error ranges observed in our study were comparable to former studies for DS DECT [2, 17, 21, 22, 27], SS DECT using a split filter [19], and DL DECT [23]. To date, there are only a few studies assessing the accuracy of SS fast kV-switching DECT, which report contradictory results with smaller [28, 29] or higher measurement errors compared to our results [20]. We hypothesise that these discrepancies are due to major differences in study design and scan setups.

Several potential limitations of our study merit consideration. First, we limited our investigation to a phantom study and, thus, our results may differ slightly in actual patients. We believe that a clinical study assessing the measurement errors of DECT-IQ is hardly feasible because it is impossible to know the true iodine concentration in a patient due to a lack of a gold standard. A phantom study enables the evaluation of measurement errors in a controlled environment. We hope that our results deliver the fundamentals for potential future clinical studies. Second, the scan parameters differed between the two DECT approaches and among the different pre-sets for SS DECT. We aimed to simulate a realistic clinical scenario in which the user has to choose from vendor-specific pre-sets. Third, we did not investigate higher iodine concentrations. Instead, we purposely focused on low iodine concentrations in order to calculate the minimum detectable difference in iodine concentration. Furthermore, low iodine concentrations are likely to be clinically relevant in parenchymal organs or solid lesions. Fourth, we

did not assess the full range of different strength or blending levels within the IRs. We focused on the settings that are used in routine clinical practice at our institution.

In conclusion, phantom size and radiation dose had the largest impact on the accuracy and precision of DECT-IQ. The minimum intra- and inter-conditional detectable difference in iodine concentration ranged from 0.4 to 1.5 mgI/mL. Current generations of SS and DS DECTs outperformed previous scanner generations. These results should encourage radiologists to be aware of the relatively high error ranges of DECT-IQ, especially in large-sized patients. Future clinical studies will be needed to determine if the impact of patient- and scan-related factors on DECT-IQ will influence the diagnosis and treatment of patients.

Acknowledgements We thank Cristian T. Badea and Yi Qi from the Center of In-Vivo Microscopy of Duke University Medical Center for assistance to create iodinated solutions.

Funding The authors state that this work has not received any funding.

Compliance with ethical standards

Guarantor The scientific guarantor of this publication is Dr. Andre Euler.

Conflict of interest The authors of this manuscript declare relationships with the following companies:

Rendon C. Nelson is a medical consultant to GE Healthcare.

Andre Euler is a research fellow supported by GE Healthcare and the Swiss Society of Radiology

Ehsan Samei is the recipient of research funding from Siemens Healthineers and GE Healthcare for projects unrelated to this study.

Statistics and biometry Maciej A. Mazurowski kindly provided statistical advice for this manuscript.

Informed consent Approval from the institutional animal care committee was not required because of the design as a phantom study.

Ethical approval Institutional review board approval was not required because of the design as a phantom study.

Methodology
- prospective
- experimental
- performed at one institution

References

1. Graser A, Becker CR, Staehler M et al (2010) Single-phase dual-energy CT allows for characterization of renal masses as benign or malignant. Invest Radiol 45:399–405
2. Chandarana H, Megibow AJ, Cohen BA et al (2011) Iodine quantification with dual-energy CT: phantom study and preliminary experience with renal masses. AJR Am J Roentgenol 196:W693–W700
3. Song KD, Kim CK, Park BK, Kim B (2011) Utility of iodine overlay technique and virtual unenhanced images for the characterization of renal masses by dual-energy CT. AJR Am J Roentgenol 197:W1076–W1082
4. Ascenti G, Mileto A, Krauss B et al (2013) Distinguishing enhancing from nonenhancing renal masses with dual-source dual-energy CT: iodine quantification versus standard enhancement measurements. Eur Radiol 23:2288–2295
5. Dai X, Schlemmer HP, Schmidt B et al (2013) Quantitative therapy response assessment by volumetric iodine-uptake measurement: initial experience in patients with advanced hepatocellular carcinoma treated with sorafenib. Eur J Radiol 82:327–334
6. Mileto A, Marin D, Ramirez-Giraldo JC et al (2014) Accuracy of contrast-enhanced dual-energy MDCT for the assessment of iodine uptake in renal lesions. AJR Am J Roentgenol 202:W466–W474
7. Chang S, Hur J, Im DJ et al (2016) Dual-energy CT-based iodine quantification for differentiating pulmonary artery sarcoma from pulmonary thromboembolism: a pilot study. Eur Radiol 26:3162–3170
8. Martin SS, Weidinger S, Czwikla R et al (2018) Iodine and fat quantification for differentiation of adrenal gland adenomas from metastases using third-generation dual-source dual-energy computed tomography. Invest Radiol 53:173–178
9. Rizzo S, Radice D, Femia M et al (2018) Metastatic and non-metastatic lymph nodes: quantification and different distribution of iodine uptake assessed by dual-energy CT. Eur Radiol 28:760–769
10. Fan S, Li X, Zheng L, Hu D, Ren X, Ye Z (2017) Correlations between the iodine concentrations from dual energy computed tomography and molecular markers Ki-67 and HIF-1alpha in rectal cancer: a preliminary study. Eur J Radiol 96:109–114
11. Li J, Fang M, Wang R et al (2018) Diagnostic accuracy of dual-energy CT-based nomograms to predict lymph node metastasis in gastric cancer. Eur Radiol. https://doi.org/10.1007/s00330-018-5483-2
12. Baxa J, Matouskova T, Krakorova G et al (2016) Dual-phase dual-energy CT in patients treated with Erlotinib for advanced non-small cell lung cancer: possible benefits of iodine quantification in response assessment. Eur Radiol 26:2828–2836
13. Hellbach K, Sterzik A, Sommer W et al (2017) Dual energy CT allows for improved characterization of response to antiangiogenic treatment in patients with metastatic renal cell cancer. Eur Radiol 27:2532–2537
14. Marin D, Davis D, Roy Choudhury K et al (2017) Characterization of small focal renal lesions: diagnostic accuracy with single-phase contrast-enhanced dual-energy ct with material attenuation analysis compared with conventional attenuation measurements. Radiology 284:737–747
15. Mileto A, Marin D, Alfaro-Cordoba M et al (2014) Iodine quantification to distinguish clear cell from papillary renal cell carcinoma at dual-energy multidetector CT: a multireader diagnostic performance study. Radiology 273:813–820
16. Feuerlein S, Heye TJ, Bashir MR, Boll DT (2012) Iodine quantification using dual-energy multidetector computed tomography imaging: phantom study assessing the impact of iterative reconstruction schemes and patient habitus on accuracy. Invest Radiol 47:656–661
17. Koonce JD, Vliegenthart R, Schoepf UJ et al (2014) Accuracy of dual-energy computed tomography for the measurement of iodine concentration using cardiac CT protocols: validation in a phantom model. Eur Radiol 24:512–518
18. Faby S, Kuchenbecker S, Sawall S et al (2015) Performance of today's dual energy CT and future multi energy CT in virtual non-contrast imaging and in iodine quantification: a simulation study. Med Phys 42:4349–4366

19. Euler A, Parakh A, Falkowski AL et al (2016) Initial results of a single-source dual-energy computed tomography technique using a split-filter: assessment of image quality, radiation dose, and accuracy of dual-energy applications in an in vitro and in vivo study. Invest Radiol 51:491–498
20. Jacobsen MC, Schellingerhout D, Wood CA et al (2017) Intermanufacturer comparison of dual-energy CT iodine quantification and monochromatic attenuation: a phantom study. Radiology. https://doi.org/10.1148/radiol.2017170896:170896
21. Pelgrim GJ, van Hamersvelt RW, Willemink MJ et al (2017) Accuracy of iodine quantification using dual energy CT in latest generation dual source and dual layer CT. Eur Radiol. https://doi.org/10.1007/s00330-017-4752-9
22. Kim H, Goo JM, Kang CK, Chae KJ, Park CM (2018) Comparison of iodine density measurement among dual-energy computed tomography scanners from 3 vendors. Invest Radiol 53:321–327
23. Sauter AP, Kopp FK, Münzel D et al (2018) Accuracy of iodine quantification in dual-layer spectral CT: influence of iterative reconstruction, patient habitus and tube parameters. Eur J Radiol 102: 83–88
24. Delgado Sánchez-Gracián C, Oca Pernas R, Trinidad López C et al (2016) Quantitative myocardial perfusion with stress dual-energy CT: iodine concentration differences between normal and ischemic or necrotic myocardium. Initial experience. Eur Radiol 26:3199–3207
25. Martin SS, Czwikla R, Wichmann JL et al (2018) Dual-energy CT-based iodine quantification to differentiate abdominal malignant lymphoma from lymph node metastasis. Eur J Radiol 105:255–260
26. Kaltenbach B, Wichmann JL, Pfeifer S et al (2018) Iodine quantification to distinguish hepatic neuroendocrine tumour metastasis from hepatocellular carcinoma at dual-source dual-energy liver CT. Eur J Radiol 105:20–24
27. Li Y, Shi G, Wang S, Wang S, Wu R (2013) Iodine quantification with dual-energy CT: phantom study and preliminary experience with VX2 residual tumour in rabbits after radiofrequency ablation. Br J Radiol 86:20130143
28. Zhang D, Li X, Liu B (2011) Objective characterization of GE discovery CT750 HD scanner: gemstone spectral imaging mode. Med Phys 38:1178–1188
29. Gao SY, Zhang XY, Wei W et al (2016) Identification of benign and malignant thyroid nodules by in vivo iodine concentration measurement using single-source dual energy CT: a retrospective diagnostic accuracy study. Medicine (Baltimore) 95:e4816